

# STUDY ON THE SPATIOTEMPORAL VARIATION CHARACTERISTICS OF PRECIPITATION IN SHAANXI PROVINCE, CHINA

LI, J. B.<sup>1,2,4\*</sup> – LI, J.<sup>1,2,4</sup> – HUA, D. W.<sup>1,2,4</sup> – KONG, H.<sup>1,2,3,4</sup> – CAO, T. T.<sup>1,2,4</sup> – PANG, Z.<sup>1,2,3,4</sup> –  
JIANG, H. L.<sup>1,2,3,4</sup>

<sup>1</sup>*Shaanxi Provincial Land Engineering Construction Group Co., Ltd, Xi'an 710075, China*

<sup>2</sup>*Shaanxi Agricultural Development Group Co., Ltd., Xi'an 710075, China*

<sup>3</sup>*Shaanxi Provincial Land Consolidation Engineering Technology Research Center, Xi'an 710075, China*

<sup>4</sup>*Institute of Land Engineering and Technology, Shaanxi Provincial Land Engineering Construction Group Co., Ltd., Xi'an 710021, China*

*\*Corresponding author  
e-mail: li\_ssrs@chd.edu.cn*

(Received 17<sup>th</sup> Mar 2025; accepted 13<sup>th</sup> May 2025)

**Abstract.** This research utilizes a comprehensive combination of analytical methodologies, including linear regression, 5-year moving average, Mann-Kendall test, and R/S analysis, to examine spatiotemporal precipitation patterns across Northern Shaanxi, Guanzhong, Southern Shaanxi, and the entire province of Shaanxi from 1989 to 2023. The findings reveal notable differences in the multi-year average precipitation across different regions of Shaanxi Province. Specifically, Northern Shaanxi has an average precipitation of 481.8 mm, Guanzhong 594.9 mm, Southern Shaanxi as high as 806.6 mm, and the provincial average is 623.2 mm. All regions show an upward trend, with respective growth rates of 62.26, 52.84, 70.2, and 62.43 mm/10a for Northern Shaanxi, Guanzhong, Southern Shaanxi, and the whole province. Considering seasonal distribution, precipitation is uneven. Summer precipitation accounts for 49.13% of the annual total, making it the primary contributor to the increase in annual precipitation. The Mann-Kendall test shows that the upward trends in precipitation for Northern Shaanxi ( $\alpha = 0.01$ ), Guan-zhong ( $\alpha = 0.05$ ), Southern Shaanxi ( $\alpha = 0.01$ ), and the whole province ( $\alpha = 0.001$ ) are extremely significant, and revealed spatiotemporal heterogeneity in monthly precipitation trends, with weak declining tendencies ( $Z < 0$ ) during transitional months (January, February, March, November, December) and weak wetting signals ( $Z > 0$ ) in spring to autumn (April–October, excluding June), particularly pronounced in July and September. Moreover, R/S analysis indicates that precipitation in various regions of Shaanxi Province is likely to continue to increase in the future. In terms of spatial distribution, precipitation in the province shows a north-south gradient, with less in the north and more in the south, and pronounced seasonal variations.

**Keywords:** *Northern Shaanxi, precipitation variation, spatial-temporal distribution, Mann-Kendall test, R/S analysis*

## Introduction

Precipitation, as a core component of the water cycle, plays a pivotal role in regional water resource management, ecological sustainability, and socioeconomic development (Arab Amiri and Mesgari, 2018; Berhail and Katipoğlu, 2024; Alsubih et al., 2025). The abundance of precipitation directly influences the ebb and flow of river runoff and profoundly impacts the recharge of surface and groundwater resources. For ecosystems, precipitation is a crucial factor in maintaining vegetation growth, controlling soil erosion, and protecting biodiversity. As a major agricultural province, Shaanxi depends

highly on precipitation. The agricultural types in different regions vary due to precipitation differences. The Guanzhong Plain, with relatively moderate precipitation conditions, has become a major production area for food crops such as wheat and corn. The humid climate in Southern Shaanxi is suitable for growing water-loving crops like rice, while the semi-arid climate in Northern Shaanxi is more suitable for drought-tolerant crops such as foxtail millet and broomcorn millet. Any abnormal fluctuations in precipitation can have a significant impact on agricultural yield and quality, thus endangering regional food security (Kang et al., 2009). Therefore, in-depth research on the spatial and temporal distribution and variation characteristics of precipitation in Shaanxi Province is of great practical significance for optimizing water resource management strategies (Berhail and Katipoğlu, 2024), formulating scientific agricultural development plans, and effectively addressing the challenges of climate change (Liu et al., 2021).

Scholars in China and abroad have long been engaged in research on the spatial and temporal distribution of precipitation and its variation characteristics, and have achieved rich results. In terms of precipitation trend analysis, classic methods such as linear regression, Empirical Orthogonal Function (EOF) (Lim Kam Sian et al., 2024), and polynomial regression are widely used. Combined with Geographic Information System (GIS) technology (Arab Amiri and Mesgari, 2018; Li et al., 2023; Torelló-Sentelles et al., 2024), the spatial variation trend of precipitation can be visually presented. Ødemark et al. (2022) used the Empirical Orthogonal Function (EOF) to conduct an in-depth analysis of the long-term precipitation data from 1981 to 2018 on the west coast of Norway, revealing the regional increase and decrease trends of precipitation and their close association with the evolution of the atmospheric circulation pattern. Ullah et al. (2021) conducted an in-depth analysis of the South Asian Summer Monsoon (SASM) precipitation in Pakistan, using two methods, the Empirical Orthogonal Function (EOF) and the Percent of Normal (PN) index, to reveal the dominant spatial patterns and temporal evolution of extreme monsoon precipitation events. In the field of mutation detection, methods such as Pettitt (Svetina et al., 2024) and Mann-Kendall (Xu et al., 2024b) tests are widely applied. These methods can accurately identify the mutation points in the precipitation sequence, providing key evidence for exploring the impact of climate change on precipitation. Yan et al. (2024) based on the precipitation data from 16 rain gauge stations in the source area of the Yellow River from 1961 to 2020, applied the Pettitt test and found a mutation point between 2014-2015, with the annual precipitation change trend shifting from decreasing to increasing. Das et al. (2022) used descriptive statistical analysis and the Mann-Kendall trend test to study the changes in rainfall and temperature at all stations in Bangladesh. For cycle research, time-frequency analysis methods such as wavelet analysis (Alsubih et al., 2025) and Fourier transform (Chen et al., 2020) are dominant. With the help of these methods, the precipitation time series can be decomposed into different frequency components, revealing its periodic variation patterns at different time scales. Ren et al. (2022) analyzed and discussed the variation characteristics of precipitation in Shandong Province from 1980 to 2019 through methods such as Empirical Orthogonal Decomposition (EOF) and wavelet analysis. The results showed that the annual precipitation in Shandong Province gradually decreased from southeast to northwest and had multi-time-scale periodic characteristics.

Scholars such as Zhang et al. (2020), Xu et al. (2024a), and Cai et al. (2025) have carried out research on the analysis of precipitation variation in Shaanxi at different

time and spatial scales. However, Shaanxi Province spans multiple climate zones and has complex and diverse terrains. Although there are already some relevant research results, there are still deficiencies in the comprehensive research on precipitation at multiple scales and in different regions. Previous studies mostly focused on macro-analysis at the provincial scale or in a certain city, or on extreme precipitation analysis. Geographically, Shaanxi Province is usually divided into three regions: Northern Shaanxi, Guanzhong, and Southern Shaanxi. Northern Shaanxi includes Yulin City and Yan'an City. This area is located in the Loess Plateau and mainly has a warm-temperate semi-arid climate. The Guanzhong region includes five cities: Xi'an, Tongchuan, Baoji, Xianyang, and Weinan, and belongs to a warm-temperate semi-humid climate. The Southern Shaanxi region includes three cities: Hanzhong, Shangluo, and Ankang. It is backed by the Qinling Mountains in the north and leans against the Bashan Mountains in the south, belonging to a north-subtropical humid climate. Seasonally, it is divided into spring (March-May), summer (June-August), autumn (September-November), and winter (December-February of the following year). There is a relative lack of refined research on the monthly, seasonal, and annual scales in different regions of Northern Shaanxi, Guanzhong, and Southern Shaanxi. In view of this, based on the data from the provincial statistical yearbook, this study uses various statistical and prediction methods to conduct an in-depth analysis at multiple scales, systematically expounding the spatial and temporal variation characteristics of precipitation in Shaanxi Province, aiming to provide a scientific basis for water resource management, ecological protection, and disaster prevention and mitigation in Shaanxi Province.

## Data and methods

The meteorological data used in this study comes from the monthly precipitation data in the Shaanxi Statistical Yearbook from 1989 to 2023. The data is highly authoritative and reliable, covering 10 cities in Shaanxi Province, including different geographical regions and climate types. The precipitation is statistically analyzed on a monthly, seasonal, and annual scale. During the data collation process, the original data was carefully checked and preprocessed to ensure data integrity and accuracy. The area-weighted average method was applied to obtain the multi-year average precipitation of each region and Shaanxi Province. Methods such as linear trend analysis, moving average, R/S method, and Mann-Kendall test were used to study the spatial and temporal distribution and variation characteristics of precipitation in Shaanxi Province.

## Results and analysis

### *Analysis of precipitation variation trends*

Linear fitting and 5-year moving average were used to analyze the trend of the dynamic changes in the multi-year precipitation in Northern Shaanxi, Guanzhong, Southern Shaanxi, and Shaanxi, respectively. The results are shown in *Figure 1*. There are significant differences in the multi-year precipitation in different regions of Shaanxi Province. The multi-year average precipitation in Northern Shaanxi, Guanzhong, Southern Shaanxi, and Shaanxi is 481.8 mm, 594.9 mm, 806.6 mm, and 623.2 mm, respectively. According to the least-squares fitting results, the precipitation in all regions shows an increasing trend, rising at a rate of 62.26 mm/10a, 52.84 mm/10a,

70.2 mm/10a, and 62.43 mm/10a, respectively, and the trend is not significant. The 5-year moving average lines of precipitation in Northern Shaanxi and the whole province were both higher than the average precipitation after, 2012 and 2010, respectively.

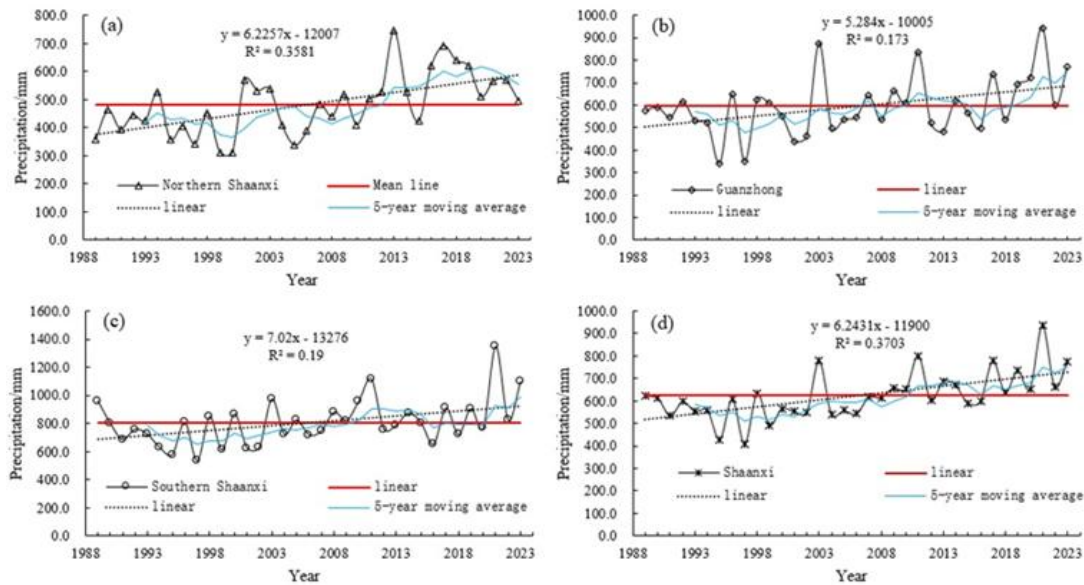


**Figure 1.** The annual average precipitation variation in Shaanxi province from 1989 to 2023

Table 1 shows the coefficient of variation ( $C_v$ ) of precipitation in Shaanxi Province and its regions, which reflects the relative dispersion degree of the data, that is, the degree of data fluctuation relative to its average level. The larger the coefficient of variation, the greater the data fluctuation. As can be seen from Table 1, the coefficient of variation of precipitation in Northern Shaanxi is the largest, at 22.13%, indicating that the precipitation in this region fluctuates violently. Followed by Guanzhong and Southern Shaanxi. From the perspective of the whole province, the coefficient of variation is relatively small, only 16.87%, indicating that the precipitation in the whole province fluctuates less compared with that in each region.

**Table 1.** The coefficient of variation for long-term precipitation in Shaanxi Province

Project	Northern Shaanxi	Guanzhong	Southern Shaanxi	Shaanxi
Coefficient of variation ( $C_v$ )	22.13%	21.88%	20.46%	16.87%

Table 2 shows the average value, proportion, correlation coefficient, linear change rate, and coefficient of variation of precipitation in each season in Shaanxi Province in the past 35 years. Precipitation in the whole province is mainly concentrated in summer, accounting for 49.13%, while the precipitation in winter is the least, only 3.36%. According to the least-squares linear fitting results, the linear relationship of precipitation in summer and autumn is relatively strong, while that in winter is relatively weak. At the same time, the precipitation in spring, summer, and autumn all shows an increasing trend, and the increasing trend in autumn is the largest, reaching 31.723 mm/10a. The precipitation in winter shows a decreasing trend, with a small

change rate of only -0.201 mm/10a. Combining the average seasonal precipitation and the change rate, the increase in summer precipitation is the main reason for the increase in the annual precipitation in Shaanxi Province. From the coefficient of variation, the coefficient of variation value in winter is the largest, and the precipitation fluctuates most violently. Followed by autumn, and the coefficient of variation in summer is the smallest, only 0.1774, indicating that the precipitation fluctuation is relatively gentle.

**Table 2.** The coefficient of variation for long-term precipitation in Shaanxi Province

Parameter	Spring	Summer	Autumn	Winter
Average seasonal precipitation (mm)	120.6	306.1	175.4	20.9
Proportion of multi-year average precipitation (%)	19.36	49.13	28.15	3.36
Correlation coefficient (R)	0.1954	0.4553	0.4590	0.02
Change rate (mm/10a)	6.866	24.132	31.723	-0.201
Coefficient of variation (Cv)	0.2985	0.1774	0.4037	0.5052

Figure 2 shows the distribution of monthly average precipitation in Shaanxi Province and its regions. Precipitation in Northern Shaanxi, Guanzhong, and Southern Shaanxi all shows a single-peak form within the year, and the peak value appears from July to September. The highest precipitation is in Southern Shaanxi, which occurs in July, reaching 139.4 mm. Followed by Northern Shaanxi, which occurs in August, reaching 113.2 mm. In Guanzhong, it occurs in September, reaching 103.8 mm. The precipitation in Northern Shaanxi, Guanzhong, and Southern Shaanxi is mainly concentrated from July to September, accounting for 60.1%, 50.2%, and 49.4% of their respective annual precipitation. The precipitation in January, February, and December is relatively small, accounting for 2.7%, 4.1%, and 3.5% of their respective annual precipitation. From the perspective of the whole province, the precipitation peak appears in July, and the precipitation from July to September accounts for 52.8% of the whole year.

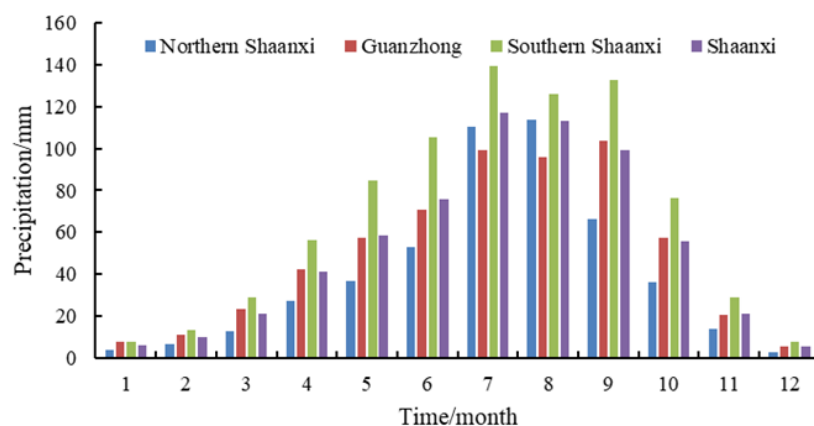


**Figure 2.** Annual distribution of average monthly precipitation in Shaanxi from 1989 to 2023

As can be seen from Figure 3, the multi-year average precipitation and the precipitation in each season in Northern Shaanxi, Guanzhong, and Southern Shaanxi are all the highest in Southern Shaanxi, accounting for 34.6%, 30.3%, 33.4%, and 32.8% of each season, respectively. Except that the precipitation in summer in Guanzhong is the

least, at 266.3 mm, the precipitation in the remaining seasons is the least in Northern Shaanxi. In Northern Shaanxi, Guanzhong, Southern Shaanxi, and the whole province, the precipitation in summer is the most in the four seasons, all above 260 mm, and the least in winter, all not higher than 30 mm. The precipitation in spring in Northern Shaanxi is relatively small, only 76.2 mm, and the impact of spring drought on crops needs to be considered. While the precipitation in summer in Southern Shaanxi is relatively high, reaching 370.8 mm, and the prevention of flood disasters needs to be considered.

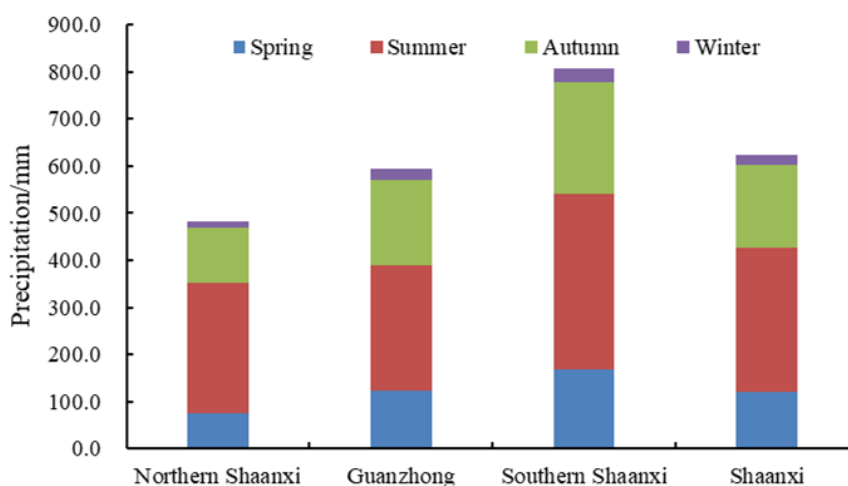


**Figure 3.** Seasonal precipitation distribution in different regions of Shaanxi from 1989 to 2023

### ***M-K test and mutation analysis of precipitation***

The Mann-Kendall test method was used to conduct trend tests and mutation analyses on the precipitation in Northern Shaanxi, Guanzhong, Southern Shaanxi, and the whole province from 1989 to 2023 (*Table 3; Fig. 4*). The critical values at the 95%, 99%, and 99.9% confidence levels are 1.96, 2.576, and 3.291, respectively. As can be seen from *Table 3*, the Z-value of precipitation in Northern Shaanxi, Guanzhong, Southern Shaanxi, and the whole province are all greater than zero, indicating that the precipitation has an upward trend, and the upward trend is significant at the significance levels of  $\alpha = 0.01$ ,  $\alpha = 0.05$ ,  $\alpha = 0.01$ , and  $\alpha = 0.001$ , respectively.

**Table 3.** The precipitation Z value of Shaanxi province

Project	Northern Shaanxi	Guanzhong	Southern Shaanxi	Shaanxi
Z value	3.266**	2.045*	2.386**	3.636***

1 \*, \*\*, \*\*\* represent  $\alpha = 0.05$ , 0.01, 0.001, respectively

In *Figure 4*, if  $UF > 0$ , it indicates that the sequence has an upward trend, and vice versa. When the UF value exceeds the critical line, it indicates that the upward or downward trend is significant, and the part exceeding the critical line is the area where the mutation occurs. If there is an intersection between UF and UB, and the intersection is between the critical lines, the time corresponding to the intersection is the starting time of the mutation. According to *Figure 4*, the UF curve in Northern Shaanxi fluctuated frequently before 2007, showing an up-down-up-down change, and then

maintained an upward trend. Since 2016, the absolute value of the UF curve has been greater than 1.96, indicating that the precipitation shows a significant upward trend. There is no intersection between the UF and UB curves, indicating that there is no clear starting time of mutation in precipitation from 1989 to 2023. The UF curve in the Guanzhong region fluctuated in the early stage, showing a downward trend basically from 1993 to 2009, and then an upward trend from 2009. In 2023, the trend became significant. Within the critical lines ( $\pm 1.96$ ), there are two intersections between the UF and UB curves around 1995, indicating that the sequence has experienced two state changes. The UF curve in Southern Shaanxi was less than zero before 2005, indicating that the precipitation in this region showed a downward trend during this period, and then has been showing an upward trend. Since 2021, the upward trend has been significant. There are multiple intersections between the UF and UB curves during the downward process, indicating that multiple mutations have occurred. From the perspective of the whole province, the precipitation showed a decreasing trend before 2008 and then an increasing trend. Since 2017, the precipitation has shown a significant increasing trend, and two mutations occurred between 1989 and 1993.

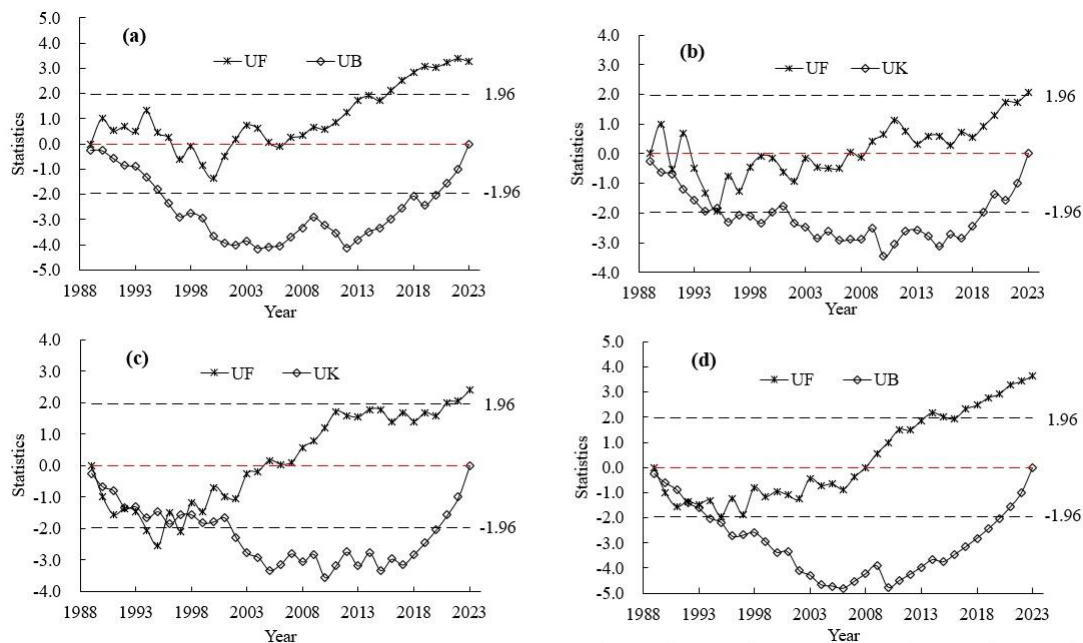


**Figure 4.** M-K mutation test of annual precipitation in Shaanxi Province from 1989 to 2023. (a) represent Northern Shaanxi, (b) represent Guanzhong, (c) represent Southern Shaanxi, (d) represent the whole Shaanxi province

In Table 4, revealed monthly precipitation trends characterized by negative Z-values ( $Z < 0$ ) in January, February, March, June, November, and December, indicating a weak declining tendency in rainfall, though these trends were statistically insignificant ( $p > 0.05$ ). Conversely, positive Z-values ( $Z > 0$ ) were observed from April to October (except June), with July and September showing more pronounced wetting signals, yet all upward trends similarly lacked statistical significance at the 95% confidence level. This spatial-temporal pattern suggests intra-annual heterogeneity in precipitation dynamics, with transitional seasons exhibiting contrasting hydrological behaviors.

In *Figure 5*, the UF curve in January fluctuated around 0, indicating an unstable precipitation trend. In February, the UF curve has fluctuated around -1.96 in recent years, indicating a downward trend in precipitation. The UF curve in March, April, and May has shown an upward trend in recent years. In June and November, the UF curve has approached the critical line of 1.96, indicating an increasing trend in precipitation in the short term. The UF curve for July, August, and September mostly remained above 0, indicating an increasing trend in precipitation, but not significant. The UF curve in December mostly falls between 0 and -1.96, indicating an insignificant downward trend in precipitation. There are no mutation points in September, but there are one or more mutation points in other months.

### ***R/S analysis of precipitation***

According to the principle of *R/S* analysis, a univariate linear regression was performed on  $\lg(R/S)$  and  $\lg(i)$  to obtain the Hurst exponent *H*-value (Chandrasekaran et al. 2019), so as to judge the future change trend based on the historical change trend of annual precipitation in each region. The results are shown in *Figure 6*. The *H*-value is between 0 and 1. When  $H = 0.5$ , it indicates that all indicators are completely independent; when  $0.5 < H < 1$ , it indicates that the time series has persistence, and the future trend is consistent with the past; when  $0 < H < 0.5$ , it indicates that the future trend is opposite to the past (Lin et al. 2024). The *H*-values of the precipitation time series in Northern Shaanxi, Guanzhong, Southern Shaanxi, and the whole province are all greater than 0.5, indicating that there is a relatively obvious Hurst phenomenon in the precipitation of each region. The possibility that the future precipitation will continue the past precipitation is relatively high. Especially, the *H*-value of Northern Shaanxi reaches 0.9016, showing a stronger continuity. Therefore, it can be predicted that the precipitation in Northern Shaanxi, Guanzhong, Southern Shaanxi, and the whole province will probably continue to increase in the future.

### ***Spatial distribution characteristics of precipitation***

*Figure 7* shows the distribution of the multi-year average precipitation and the multi-year average precipitation in each season in the cities of Shaanxi Province. The spatial distribution of the multi-year average precipitation in Shaanxi Province is uneven, showing an overall trend of less in the north and more in the south, and more in the west and less in the east in the southern part. Among them, the multi-year average precipitation in Yulin is the lowest in the province, only 430.5 mm, while that in Hanzhong is as high as 850.2 mm, with a significant gap between the two places. In terms of seasons, there is a significant difference in precipitation between the north and the south in spring. The precipitation in the north is obviously scarce, while that in the south is relatively abundant. The spring precipitation in Yulin is as low as 66.9 mm, while that in Ankang reaches 181.4 mm, nearly three times that of Yulin. The distribution pattern of summer precipitation is rather special, showing less in the middle, more in the south, and concentrated in the north, but the gap between the middle and the north is small. Among them, the summer precipitation in Xianyang is the least, 236.4 mm, and that in Ankang is the most, 397.0 mm, almost 1.7 times that of Xianyang. Autumn precipitation continues the characteristic of less in the north and more in the south. Yulin has the lowest precipitation in the province with 97.7 mm, while Hanzhong ranks first with 262.6 mm. In winter, the precipitation in the whole province is generally scarce, all less than 32 mm,

still following the law of less in the north and more in the south. Yulin has only 10.7 mm, and Shangluo has relatively the most, but only 31.4 mm.

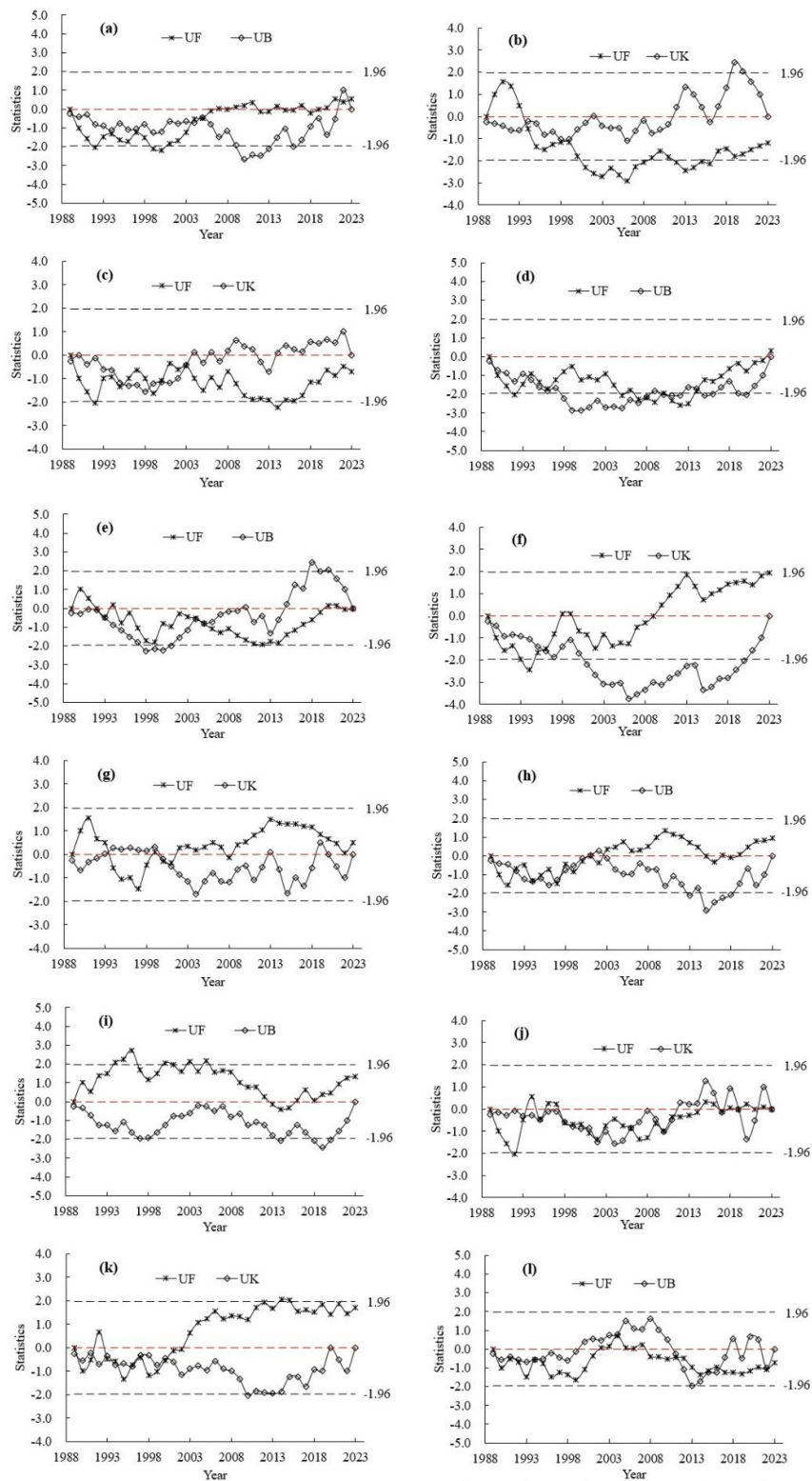


**Figure 5.** Monthly precipitation M-K mutation test of Shaanxi Province from 1989 to 2023. (a) to (l) represent the precipitation in January, February, March, April, May, June, July, August, September, October, November and December respectively

**Table 4.** Monthly precipitation Z value of Shaanxi province

Project	January	February	March	April	May	June
Z value	-0.710	-0.540	-1.193	0.284	0.483	-0.028
Project	July	August	September	October	November	December
Z value	1.931	0.909	1.704	1.307	-0.028	-0.739

1 \*, \*\*, \*\*\* represent  $\alpha = 0.05, 0.01, 0.001$ , respectively

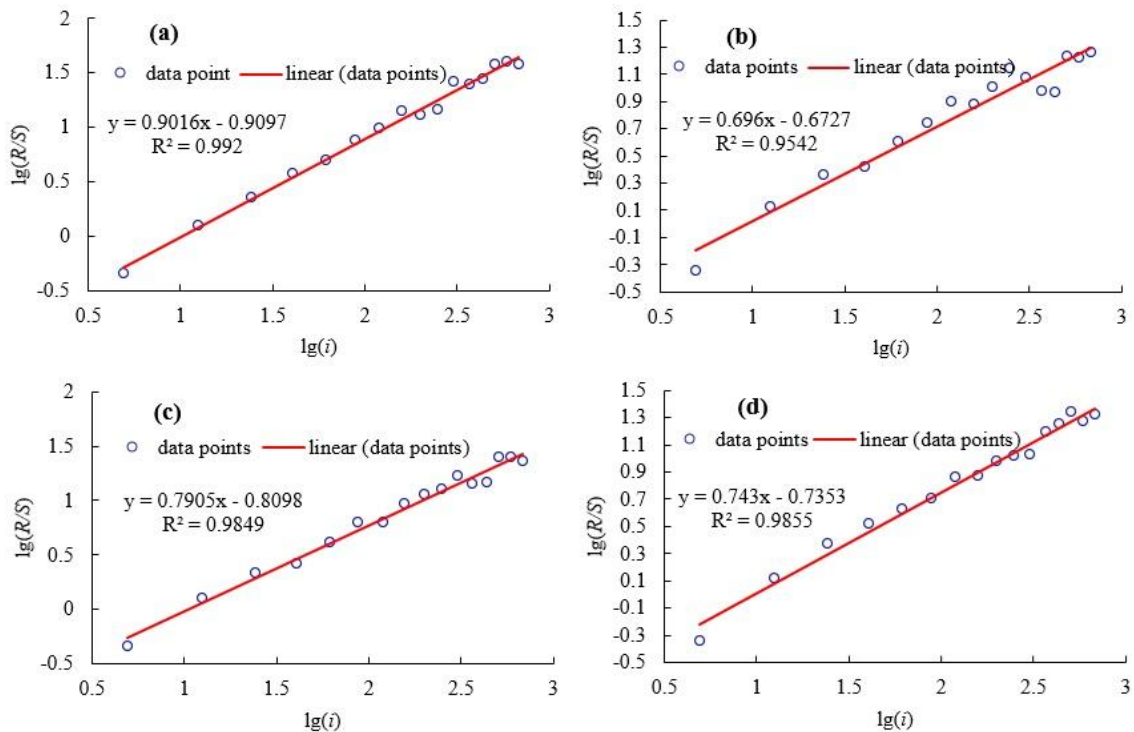


**Figure 6.** The  $i \sim R/S$  relationship of precipitation in Shaanxi Province from 1989 to 2023. (a) represent Northern Shaanxi, (b) represent Guanzhong, (c) represent Southern Shaanxi, (d) represent the whole Shaanxi province

## Discussion

The findings reveal significant north-south disparities and seasonal differentiation in precipitation patterns across Shaanxi Province. Annual precipitation in southern Shaanxi (806.6 mm) substantially exceeds that of northern Shaanxi (481.8 mm), with summer rainfall accounting for nearly 50% of total precipitation, aligning with China's characteristic "southern flood-northern drought" pattern (Huangfu et al., 2015; Wang et al., 2021a). Northern Shaanxi exhibits a notably higher precipitation coefficient of variation (22.13%) compared to the provincial average (16.87%), indicating intensified rainfall variability likely attributable to combined topographic effects and monsoon marginal zone influences. Situated in the northern Loess Plateau, this region experiences amplified interannual precipitation fluctuations due to alternating controls between westerlies and East Asian monsoons (Wang et al., 2021b). Although provincial annual precipitation demonstrates an increasing trend (62.26–70.2 mm/decade), the linear trends remain statistically insignificant ( $\alpha > 0.05$ ), consistent with the warming

hiatus in northern China precipitation observed in IPCC AR6, potentially modulated by natural climate variability.

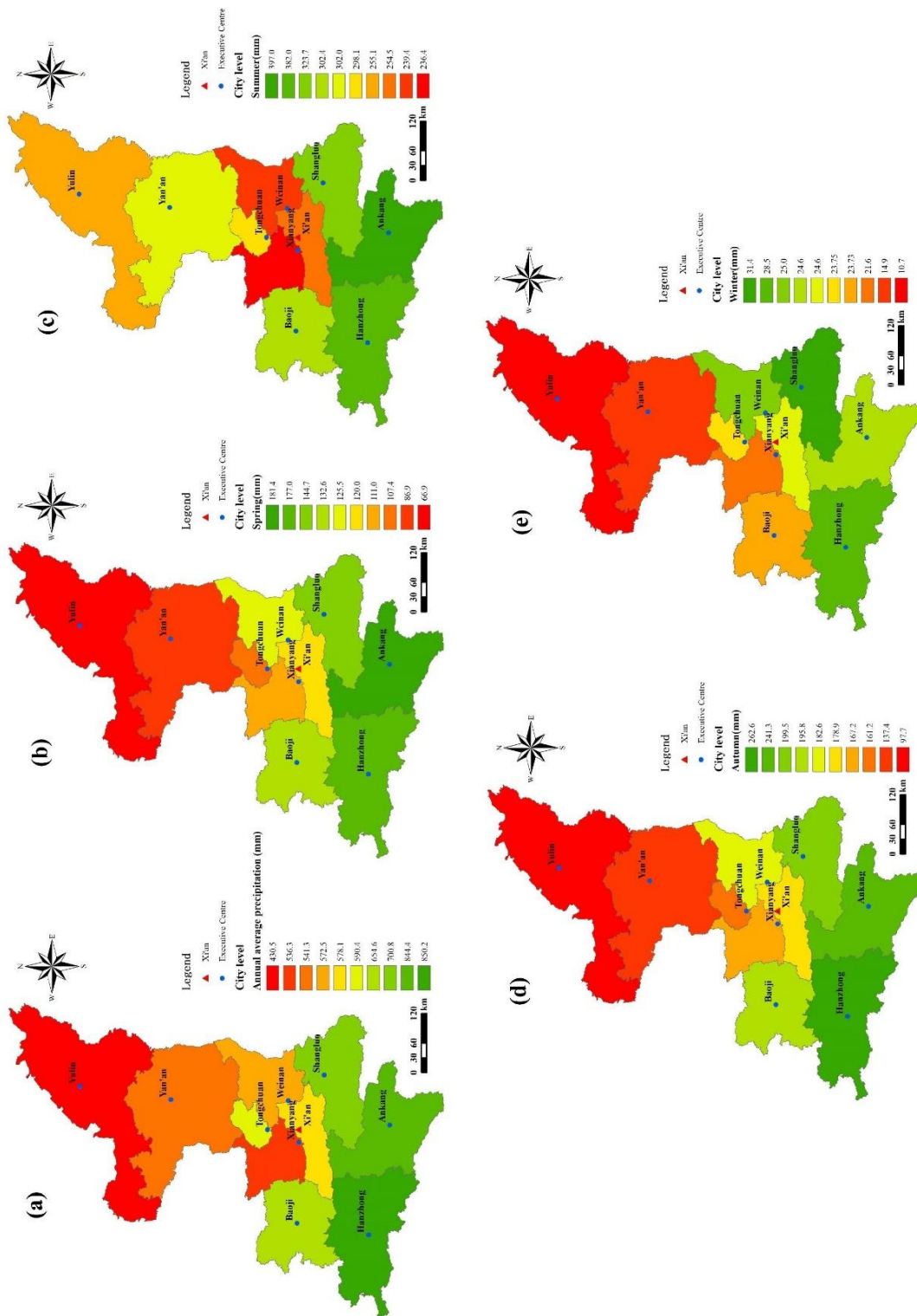


**Figure 7.** Map of the long-term average annual and seasonal precipitation distribution in various cities of Shaanxi Province from 1989 to 2023. (a) represent annual average precipitation, (b), (c), (d) and (e) represent the annual average precipitation in spring, summer, autumn and winter respectively

Seasonal analysis shows pronounced summer precipitation concentration (49.13%) with significant growth (24.132 mm/decade), contrasting with winter precipitation decline (-0.201 mm/decade), exacerbating seasonal distribution imbalances. Similar studies in North China associate increasing summer rainfall proportions with enhanced East Asian summer monsoon intensity (Liu et al., 2020). Spring and autumn precipitation increases (6.866–31.723 mm/decade) may reflect synergistic effects between intensified evaporation and altered moisture transport pathways under climate warming. Monthly distribution highlights July–September dominance (52.8% of annual precipitation), coinciding with Shaanxi’s critical flood season (“late July to early August”), necessitating enhanced extreme precipitation monitoring. Mann-Kendall tests detect significant post-2016 precipitation intensification in northern Shaanxi, Guanzhong region, and province-wide ( $Z > 1.96$ ), corresponding to abrupt change windows in northern China precipitation under global warming (Li et al., 2020). R/S analysis identifies the highest Hurst index in northern Shaanxi (0.9016), suggesting persistent precipitation increases, consistent with CMIP6 model projections (Xu et al., 2022).

Spatial heterogeneity manifests a distinct south-north precipitation gradient (Hanzhong: 850.2 mm vs. Yulin: 430.5 mm), primarily governed by the Qinling Mountains’ orographic lifting effects. Summer precipitation dominance in annual totals and its increasing trend constitute key drivers of provincial precipitation enhancement, aligning with monsoon climate dynamics where summer monsoon intensity dictates rainfall distribution (Zhou et al., 2021; Zhao et al., 2023; Du et al., 2024). Despite elucidating spatiotemporal precipitation characteristics, limitations persist: monthly statistical data may obscure daily extreme events, and urban-centered station networks inadequately capture mountain precipitation. Future research should integrate reanalysis data with machine learning to disentangle anthropogenic impacts and validate Hurst index extrapolations through extended observational records.

## Conclusion

This study systematically elucidates the spatiotemporal evolution patterns of precipitation in Shaanxi Province from 1989 to 2023. Through multi-method fusion analysis, it clarifies the persistence, phase characteristics, and spatial heterogeneity of precipitation changes. Key findings reveal that the annual mean precipitation in Shaanxi has increased significantly at 62.43 mm/decade, with summer rainfall contributing 49.13% of total precipitation. Autumn demonstrates the most substantial increase (31.723 mm/decade), while winter shows a slight declining trend (-0.201 mm/decade). Spatially, the “north-south disparity” pattern persists, with marked differences between Yulin (430.5 mm) and Hanzhong (850.2 mm). R/S analysis uncovered strong persistence in precipitation sequences (Hurst index  $H > 0.5$ ), predicting continued increases in northern Shaanxi ( $H = 0.9016$ ), Guanzhong, and southern regions. M-K test further identified critical transition points, including dual mutation of precipitation state in Guanzhong (1995) and province-wide trend reversal (2008), and revealed spatial-temporal heterogeneity in monthly precipitation trends, characterized by weak declining tendencies ( $Z < 0$ ) in transitional months (January, February, March, November, December) and wetting signals ( $Z > 0$ ) in spring to autumn (April–October, excluding June), with July and September showing relatively stronger trends. However, all trends remained statistically insignificant ( $p > 0.05$ ) at the 95% confidence level.

These outcomes provide scientific foundations for regional water resource management, drought-flood disaster prevention, and ecological conservation. However, constrained by data timeliness and mechanistic interpretation depth, future research should integrate climate models with high-resolution data, employ numerical simulations to quantify interactions between atmospheric circulation and anthropogenic activities, and comprehensively assess precipitation impacts on regional water resources, ecosystems, and socio-economic systems. Such advancements will offer more holistic scientific support for sustainable regional development.

**Funding.** This research was funded by Shaanxi Province key research and development Plan-key industrial chain project (2022ZDLNY02-04), Shaanxi Province Land Engineering Construction Group Internal Scientific Research Project (DJNY2024-27) and Technology Innovation Center for Land Engineering and Human Settlements, Shaanxi Land Engineering Construction Group Co., Ltd and Xi'an Jiaotong University (2024WHZ0243).

## REFERENCES

- [1] Alsubih, M., Mallick, J., Alqadhi, S., Hang, H. T. (2025): Spatiotemporal analysis of drought severity and vegetation health using wavelet coherence: a case study in arid regions of Saudi Arabia. – *Theoretical and Applied Climatology* 156: 159. 10.1007/s00704-025-05390-6.
- [2] Arab Amiri, M., Mesgari, S. (2018): Analyzing the spatial variability of precipitation extremes along longitude and latitude, northwest Iran. – *Kuwait Journal of Science* 45.
- [3] Berhail, S., Katipoğlu, O. M. (2024): Exploring hydrological and meteorological drought trends in Northeast Algeria: implications for water resource management. – *Theoretical and Applied Climatology* 155: 9689-9712. 10.1007/s00704-024-05207-y.
- [4] Cai, X., Cai, Y., Ye, D., Li, Q., Hu, Y., Hu, L. (2025): Spatial and temporal variations of heavy precipitation with different durations during warm season in Shaanxi Province from 1981 to 2020. – *Arid Land Geography* 48: 1-10.
- [5] Chandrasekaran, S., Poomalai, S., Saminathan, B., Suthanthiravel, S., Sundaram, K., Abdul Hakkim, F. F. (2019): An investigation on the relationship between the Hurst exponent and the predictability of a rainfall time series. – *Meteorological Applications* 26: 511-519. <https://doi.org/10.1002/met.1784>.
- [6] Chen, Z., Hu, Q., Yong, B., Li, L., Wang, Y. (2020): Validation of precipitation spatial variogram based on fast Fourier transformation. – *Water Resources Protection* 36: 22-27.
- [7] Das, L. C., Mohiul Islam, A. S. M., Ghosh, S. (2022): Mann–Kendall trend detection for precipitation and temperature in Bangladesh. – *International Journal of Big Data Mining for Global Warming* 04: 2250001. 10.1142/s2630534822500012.
- [8] Du, Y., Li, S., Feng, D., Xiao, Y., Chen, X., Huang, S., Du, L. (2024): Characteristics of extreme summer precipitation and large-scale circulation in Shaanxi Province under global warming. – *Plateau Meteorology* 43: 342-352.
- [9] Huangfu, Jing Liang, Hui, H. R., Chen, Wen (2015): Influence of tropical western Pacific warm pool thermal state on the interdecadal change of the onset of the South China Sea summer monsoon in the late-1990s. – *Atmospheric and Oceanic Science Letters* 8: 95-99. 10.3878/AOSL20150002.
- [10] Kang, Y., Khan, S., Ma, X. (2009): Climate change impacts on crop yield, crop water productivity and food security—a review. – *Progress in Natural Science* 19: 1665-1674. <https://doi.org/10.1016/j.pnsc.2009.08.001>.

- [11] Li, L., Xiao, Z., Luo, S., Yang, A. (2020): projected changes in precipitation extremes over Shaanxi Province, China, in the 21st century. – *Advances in Meteorology* 2020: 1808404. <https://doi.org/10.1155/2020/1808404>.
- [12] Li, N. N., Chen, X. H., Qiu, J., Li, W. H., Zhao, B. K. (2023): Spatio-temporal characteristics and trend prediction of extreme precipitation—taking the Dongjiang River basin as an example. – *Water* 15: 2171.
- [13] Lim Kam Sian, K. T. C., Sagero, P., Ongoma, V. (2024): Precipitation, temperature and potential evapotranspiration for 1991–2020 climate normals over Africa. – *Theoretical and Applied Climatology* 155: 5465-5482. 10.1007/s00704-024-04963-1.
- [14] Lin, D. R., Zhong, W., Wang, X. J., Quan, M. Y., Li, T. H., Zhang, E. L. (2024): Spatiotemporal characteristics and forcing mechanism of precipitation changes in the Nanling Mountains and surrounding regions in South China over the past 60 years. – *Theoretical and Applied Climatology* 156: 57. 10.1007/s00704-024-05287-w.
- [15] Liu, H., Miao, J., Wu, K., Du, M., Zhu, Y., Hou, S. (2020): Why the increasing trend of summer rainfall over North China has halted since the Mid-1990s. – *Advances in Meteorology* 2020: 9031796. <https://doi.org/10.1155/2020/9031796>.
- [16] Liu, L. Y., Lu, R. J., Ding, Z. Y., Wang, L. X., Liu, X. K. (2021): Analysis of climate change characteristics and circulation factors in the Loess Plateau. – *Journal of Earth Environment* 12: 615-631.
- [17] Ødemark, K., Müller, M., Tveito, O., Palerme, C. (2022): Recent changes in circulation patterns and their opposing impact on extreme precipitation at the west coast of Norway. – *Weather and Climate Extremes* 39: 100530. 10.1016/j.wace.2022.100530.
- [18] Ren, J., Wang, F., Lu, X. (2022): Characteristics of spatiotemporal variation of annual precipitation in Shandong Province based on EOF and wavelet analysis. – *Research of Soil and Water* 29: 179-183. 10.13869/j.cnki.rswc.2022.02.030.
- [19] Svetina, J., Prestor, J., Jamnik, B., Auersperger, P., Brenčič, M. (2024): Contaminant trends in urban groundwater: case study from Ljubljana (Central Slovenia). – *Water* 16: 890.
- [20] Torelló-Sentelles, H., Marra, F., Koukoula, M., Villarini, G., Peleg, N. (2024): Intensification and changing spatial extent of heavy rainfall in urban areas. – *Earth's Future* 12 10.1029/2024EF004505.
- [21] Ullah, W., Wang, G., Lou, D., Ullah, S., Bhatti, A. S., Ullah, S., Karim, A., Hagan, D. F. T., Ali, G. (2021): Large-scale atmospheric circulation patterns associated with extreme monsoon precipitation in Pakistan during 1981–2018. – *Atmospheric Research* 253: 105489. <https://doi.org/10.1016/j.atmosres.2021.105489>.
- [22] Wang, L., Chen, S., Zhu, W., Ren, H., Zhang, L., Zhu, L. (2021a): Spatiotemporal variations of extreme precipitation and its potential driving factors in China's North-South Transition Zone during 1960–2017. – *Atmospheric Research* 252: 105429. <https://doi.org/10.1016/j.atmosres.2020.105429>.
- [23] Wang, Y., Tan, D., Han, L., Li, D., Wang, X., Lu, G., Lin, J. (2021b): Review of climate change in the Yellow River Basin. – *Journal of Desert Research* 41: 235-246. 10.7522/j.issn.1000-694X.2021.00086.
- [24] Xu, H., Chen, H., Wang, H. (2022): Future changes in precipitation extremes across China based on CMIP6 models. – *International Journal of Climatology* 42: 635-651. <https://doi.org/10.1002/joc.7264>.
- [25] Xu, J., Tian, T., Zhang, Y. D. (2024a): Analysis on characteristics and impact of spatial and temporal variations of precipitation in Shaanxi Province. – *Sichuan Environment* 43: 7-15. 10.14034/j.cnki.schj.2024.04.002.
- [26] Xu, J., Zhao, Y., Chen, Y., Du, P., Qu, L. (2024b): Hydrological changes and sediment dynamics in the Inner Mongolia section of the Yellow River: implications for reservoir management. – *Water* 16: 810.
- [27] Yan, C., Wang, P., Jin, L., Liu, J., Xuan, D., Zhang, R. (2024): Research on the temporal and spatial variation characteristics of precipitation in the source region of the Yellow

- River from 1961 to 2020. – *Journal of China Hydrology* 44: 84-91. 10.19797/j.cnki.1000-0852.20230338.
- [28] Zhang, H. F., Li, J. K., Pan, L. J., Lu, S. (2020): Diurnal variation characteristics and north-south differences of precipitation in warm season in Shaanxi Province. – *Arid Land Geography* 43: 889-898.
- [29] Zhao, Z. C., Luo, Y., Huang, J. B. (2023): Global warming and floods/droughts. – *Climate Change Research* 19: 258-262.
- [30] Zhou, T. J., Chen, Z. M., Chen, X. L., Zuo, M., Jiang, J., Hu, S. (2021): Interpreting IPCC AR6: future global climate based on projection under scenarios and on near-term information. – *Climate Change Research* 17: 652-663.